Japanese Dental Science Review (2017) 53, 2—10

Contents lists available at ScienceDirect

Japanese Dental Science Review

journal homepage: www.elsevier.com/locate/jdsr

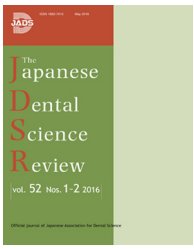

Review Article

Shedding quantitative fluorescence light on novel regulatory mechanisms in skeletal biomedicine and biodentistry

Ji-Won Lee (PhD)[a], Tadahiro Iimura (DDS, PhD)[a,b,c,*]

[a] *Division of Bio-Imaging, Proteo-Science Center (PROS), Ehime University, Ehime 791-0295, Japan*
[b] *Division of Analytical Bio-Medicine, Advanced Research Support Center (ADRES), Ehime University, Ehime 791-0295, Japan*
[c] *Artificial Joint Integrated Center and Translational Research Center, Ehime University Hospital, Ehime 791-0295, Japan*

Received 21 January 2016; received in revised form 18 April 2016; accepted 27 April 2016

KEYWORDS
Bone;
Cartilage;
Imaging;
Morphology;
Signaling

Summary Digitalized fluorescence images contain numerical information such as color (wavelength), fluorescence intensity and spatial position. However, quantitative analyses of acquired data and their validation remained to be established. Our research group has applied quantitative fluorescence imaging on tissue sections and uncovered novel findings in skeletal biomedicine and biodentistry. This review paper includes a brief background of quantitative fluorescence imaging and discusses practical applications by introducing our previous research. Finally, the future perspectives of quantitative fluorescence imaging are discussed.

Contents

1. Introduction 3
2. Confocal microscope 3
3. Image processing and quantitative analyses 3
4. Fluorescence morphometry 3

* Corresponding author at: Division of Bio-Imaging, Proteo-Science Center (PROS), Ehime University, Shitsukawa, Toon-City, Ehime 791-0295, Japan. Tel.: +81 89 960 5507; fax: +81 89 960 5052.
E-mail address: iimura@m.ehime-u.ac.jp (T. Iimura).

http://dx.doi.org/10.1016/j.jdsr.2016.04.005

5. Visualization and quantification of the cellular input levels of TGF-β and BMP signaling in cartilage development 3
6. Distinct patterns of the osteocyte network between flat and long bones 4
7. Sclerostin: a potent marker of site-specific bone metabolism 5
8. Sclerostin: a potent trigger for alveolar bone remodeling in response to orthodontic forces 6
9. DMP1: a direct negative regulator of FGF23 production by osteocytes 7
10. Morphological and functional heterogeneity of osteocytes 8
11. Future perspective 8
Conflict of interest 9
Role of funding source 9
Acknowledgements 9
References 9

1. Introduction

Undoubtedly, biologists and dental and medical scientists have long benefitted from the microscope since the initial studies of biological structures reported by pioneers such as Robert Hook and Antoni Van Leeuwenhooek in the 17th century [1—3]. The imaging quality has much improved following advances in the development of technology and manufacturing. We are standing in a historical decade of microscopic development, with the awarding of the Nobel Prize in Chemistry to Osamu Shimomura, Martin Chalfie and Roger Tsien in 2008 for the discovery and application of green fluorescent protein (GFP), and the current awarding of the Nobel Prize in Chemistry to Eric Betzig, Stefan W. Hell and William E. Moerner in 2014 for the development of super-resolution fluorescence microscopy. In this review, the application of confocal imaging and image processing in hard tissue biology is discussed by introducing our research on skeletal biology.

2. Confocal microscope

Confocal laser scanning microscopy (CSML) is designed to allow only light originating from the nominal focus to pass through a detector, such as a photomultiplier tube (PMT). To scan the specimen, a tightly focused laser is used, and the emitted light is eliminated by a pinhole placed just before the PMT, so that the image is constructed by spatially mapping the detected (well-focused) signal in accordance with the position of the scanning spot (confocality). This confocality of the scanning spot and the detected light enables the exclusion of out-of-focus blurring, thus improving the signal-to-noise ratio and image resolution.

Principally, CSLM can obtain a better resolution image than widefield fluorescence microscopy. However, to obtain a significant advantage by CSLM, the pinhole has to be closed to an extent where most of the emitted light is discarded, thus only a faint signal is detected. Therefore, for the practical use of CSLM, the pinhole must be opened even wider than the theoretically optimized size to obtain suitable images. In this case, it is extremely important to notice that the obtained signal may include some degree of out-of-focus signals.

3. Image processing and quantitative analyses

In the fluorescence microscopy system, charged-coupled devices (CCD) or photomultipliers (PMT) are used as detection apparatuses that capture visual information in a numerical form. Digitalized fluorescence images are composed of a number of pixels (or voxels in three-dimensional images) that contain numerical information such as color (wavelength), fluorescence intensity and the spatial position. By taking advantage of this digital information, reliable quantitative data can be extracted from acquired fluorescence images. Therefore, the quantitative analysis of labeled molecules or cellular functions in a spatial manner is possible, which also facilitates the comparison analysis of numerical data sets and subsequent statistical analyses. These technical advantages can be beneficial to understand a given biomedical phenomena in a compressive manner from the tissue to subcellular levels.

4. Fluorescence morphometry

Our research group has applied quantitative fluorescence imaging on histological skeletal sections by measuring the three-dimensional distributions and intensities of fluorescence signals, which is referred to as ''surface rendering'' [4—8]. Surface rendering is a common image processing method that provides the surface area, volume, signal intensity, fluorescence wavelength and spatial information of a given signal that is three-dimensionally distributed. Another image processing technique we have applied is filament tracing, which enables us to trace a network of cellular process, such as neuronal dendrites and osteocytic cellular processes, in a three-dimensional manner [4]. Using this image processing method, the number, diameter and branching number of cellular processes can be numerically scored. Therefore, we can quantitatively estimate the cellular network pattern.

5. Visualization and quantification of the cellular input levels of TGF-β and BMP signaling in cartilage development

Transforming growth factor-β (TGF-β) and Bone morphogenetic proteins (BMP) have long been described as critical growth factors of cartilage development and chondrocyte

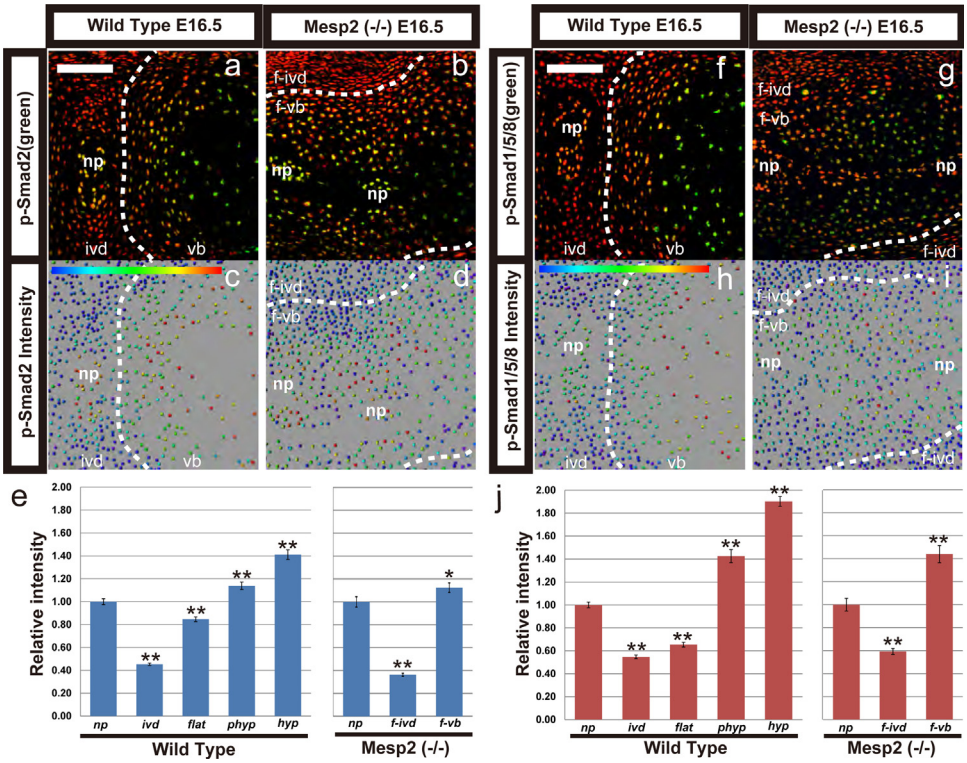

Figure 1 Quantitative three-dimensional immunofluorescence image analyses of phospho-Smad2 (a—e) and phospho-Smad1/5/8 (f—j). (a, b, f, g) Wild type and Mesp2-deficient vertebrae on E16.5. Easy 3D images of immunofluorescence against Smads (green) and nuclear staining (red). (c, d, h, i) The results of 3D spot analyses corresponding to a, b, c and d demonstrated the spatial distribution and distinct fluorescence intensities of fluorescence signals by color-coded spots. (e, j) The relative fluorescence intensities of the anti-Smads signal in distinct cartilaginous regions compared to that in nucleus pulposus cells is shown. Differentiation stages of cartilage cells such as resting, proliferative, prehypertrophic, and hypertrophic chondrocytes are morphologically determined by differential interference contrast (DIC) images of the corresponding sections. vb, vertebral body; ivd, intervertebral disk; np, nucleus pulposus; f-vb, fused vertebral body; f-ivd, fused intervertebral disk; flat, flat proliferative zone; phyp, prehypertrophic zone; hyp, hypertrophic zone.**, $p < 0.01$, $n = 4$. Scale bars (in white): 100 μm. (For interpretation of the references to color in this figure legend, the reader is referred to the web version of this article.)
Reprinted from Makino et al., 2013 [Elsevier] [6].

differentiation. A previous study has demonstrated that TGF-beta and BMP isoforms regulate immature chondrocyte proliferation and maturation (differentiation to hypertrophic chondrocyte), respectively [9—14]. However, the stage-specific cellular input levels of these growth factors in chondrocyte differentiation have not been well characterized.

To overcome this issue, we applied surface rendering of 3D fluorescence images to immunohistological sections stained with anti-phospho-Smad2 and anti-phospho-Smad1/5/8, which are major cellular effectors of TGF-β and BMP, respectively (Fig. 1) [6]. We measured the relative intensities of these signals in developing mouse vertebral cartilage. Consequently, phospho-Smad2 was increasingly detectable from the stage of flat proliferative chondrocytes to more mature chondrocytes, while phospoho-Smad1/5/8 was highly up-regulated in prehypertrophic and hypertrophic chondrocytes.

This approach can successfully visualize when, where and how much the level of TGF-β and BMP signal is activated in differentiating chondrocytes. Furthermore, this approach facilitated the evaluation of slight developmental delay and disordered cell arrangement as a phenotype of Mesp2 knockout mice, which exhibit obvious morphological disorder of the axial skeleton [6].

6. Distinct patterns of the osteocyte network between flat and long bones

Osteocytes are embedded cells in the mineralized bone matrix [15,16]. Through cellular process running throughout the osteocytic lacunar—canalicular system, each osteocyte maintains contact with other osteocytes, which comprise the cellular network throughout the bone tissue. This architectural structure also enables osteocytes to communicate with other bone cells, such as osteoclasts and osteoblasts located on the bone surface, therefore establishing a regulatory cellular network for bone metabolism.

Osteocytes are major mechanosensing cells. Therefore, it is postulated that the osteocyte network mentioned above is influenced by and adapted to distinct mechanical stimuli of attached muscle to each bone. To quantitatively address this hypothesis, we stained decalcified frozen bone sections

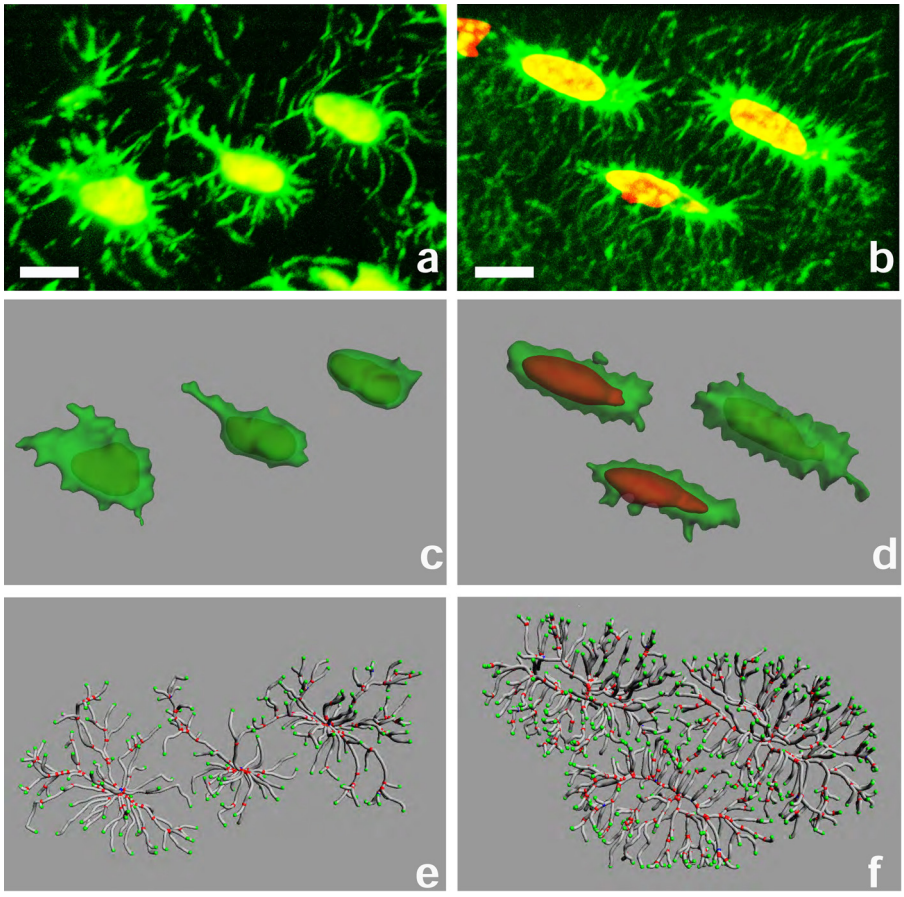

Figure 2 Three-dimensional (3D) reconstitution and surface rendering of osteocytes in the parietal bone (a, c, and e) and tibia (b, d, and f). The actin-rich cell body and cellular processes of osteocytes are visualized by a fluorescent dye-conjugated phalloidin (in green). Nuclei were counterstained by a fluorescence dye (in red). (a, b) Representative 3D-reconstituted images of the confocal z-series slices from the parietal bone (a) and tibia (b) show osteocytes and their cellular process networks. (c, d) Surface renderings of osteocyte cell bodies of the parietal bone (c) and tibia (d) from the 3D-reconstituted images (a and b, respectively) enable morphometric analyses. (e, f) Merged images of the surface renderings of cell bodies and nuclei are shown with 50% transparency of the cell bodies (in green) to visualize the relative position of the nucleus in the cell body (in red). (e, f) Dendritic tree models of the osteocytic cellular processes in the parietal bone (e) and tibia (f) from the 3D-reconstituted images (a and b, respectively). Scale bars (in white): 10 μm. (For interpretation of the references to color in this figure legend, the reader is referred to the web version of this article.)
Modified from Himeno-Ando et al., 2013 [Elsevier] [4].

with fluorescence dyes for nuclear DNA and cellular f-actin and conducted three-dimensional quantitative analyses that enabled us to measure the volumes, surface areas and shape of nuclei and cells, and the numbers of osteocytic cellular process and its branching points (Fig. 2) [4].

These analyses revealed distinct shapes of the osteocytes and complexities of the osteocyte network between flat and long bones. Specifically, in the parietal bone, osteocytes were relatively round in shape compared to tibial osteocytes, which showed a spindle shape. The relative volume of the cytoplasm in parietal osteocytes was significantly smaller than that of tibial osteocytes, although the average volume of the nuclei was not significantly different between these two populations of osteocytes. Because it is well recognized that an augmented cellular volume, which is possibly due to an increased amount of organelles such as mitochondria and ribosomes, reflects the level of cellular activity (such as energy metabolism and protein synthesis), these observations suggest that osteocytes in the long bone exhibit a more active cellular function compared to that in the flat bone. When we measured the number and complexity of the osteocyte network composed by the osteocytic cellular process, long bone osteocytes consistently showed a higher score than flat bone osteocytes. Seeing that the tibial bone is endowed with a higher level of mechanical loading than that of the parietal bone, these findings suggest that the development, maintenance and function of osteocytes and their cellular networks are mechanically adapted and exert distinct sensitivity to loading [4].

7. Sclerostin: a potent marker of site-specific bone metabolism

Sclerostin is a secreted glycoprotein that negatively regulates the proliferation and differentiation of osteoblasts,

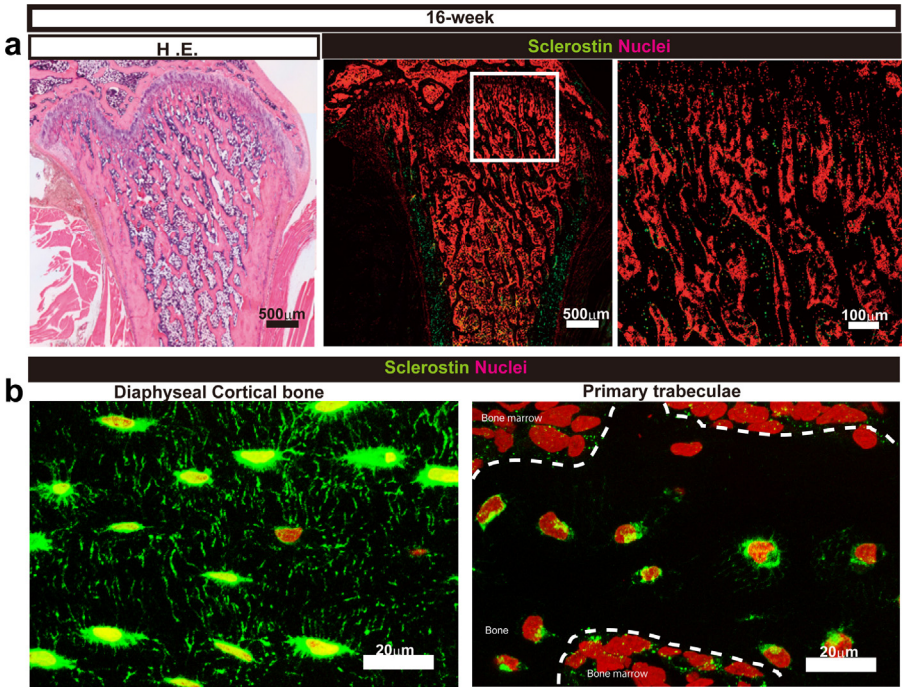

Figure 3 Confocal tiling imaging provides comprehensive views of the spatial localization of sclerostin in 16-week-old rat femurs. (a) Longitudinal serial sections were stained with hematoxylin and eosin (H.E.) (left panel), and immunostained for sclerostin (green) with nuclear counterstaining (red) (middle and right panels). Scale bars: 500 μm. (Right panel) A magnified view of the white boxed area in the middle panel is shown. White scale bar: 100 μm. (b) Confocal projection images. The dotted lines indicate the bone surface. Sclerostin and nuclei are indicated in green and red, respectively. Scale bars: 20 μm. (For interpretation of the references to color in this figure legend, the reader is referred to the web version of this article.)
Modified from Watanabe et al., 2012 [Elsevier] [8].

thus regulating bone formation through inhibiting canonical Wnt signaling [17—22]. The *SOST* gene encoding sclerostin is the responsible gene for osteosclerosis or Van Buchem disease, which are both associated with a high bone mass and dramatically thickened bone. Therefore, sclerostin is clearly a critical regulator of bone metabolism through regulating the osteoblast lineage. However, the involvement of sclerostin in pre- and postnatal bone development has remained unclear.

By obtaining whole views of bone sections with confocal tiling imaging and successive three-dimensional fluorescence morphometry for sclerostin distribution in osteocytic lacunae, we uncovered an increasing expression of sclerostin during postnatal bone development (Fig. 3) [8]. Furthermore, we observed that sclerostin is preferentially produced by cortical osteocytes, but not trabecular osteocytes. *In vitro* analyses of osteoblasts suggested that the regulatory expression of sclerostin is tightly associated with the bone formation ratio in distinct bone ages and sites. The sclerostin level was relatively low in osteocytes in bone that exert a high turnover, such as prenatal, immature postnatal bone and adult trabecular bone, while a high expression was preferentially observed in osteocytes that show a relatively low turnover, such as adult cortical bone. It is possible that highly expressed sclerostin inhibits the recruitment of osteoblast lineage cells to the bone surface, thus concomitantly and indirectly inhibiting the commitment of osteoclasts, while bone sites which express none or a small amount of sclerostin recruit and activate both osteoblast and osteocyte lineages. Therefore, sclerostin is a potential marker of site-specific bone metabolism [8].

8. Sclerostin: a potent trigger for alveolar bone remodeling in response to orthodontic forces

Osteocytes are translators of mechanical stimuli to the bone to biochemical signals that regulate the differentiation and function of other bone cells, such as osteoblasts and osteoclasts, thereby regulating bone remodeling. Sclerostin, a hallmark of osteocytes as mentioned above, is regulated by mechanical stimuli to the bone. This molecule is up- and down-regulated by unloading and loading to the bone, respectively; therefore, the expression level of this molecule may be a good marker of osteocytic responses to distinct site-specific mechanical stimuli.

Using osteocyte-ablation model mice, in which diphtheria toxin receptor-mediated cell ablation is driven by a osteocyte-specific promoter, our research group demonstrated that osteocytes played an essential role in bone resorption during orthodontic tooth movement [23]. Therefore, sclerostin was postulated to be involved in alveolar bone remodeling due to orthodontic forces.

We took advantage of multimodal confocal imaging combining zoom confocal microscopy and confocal-based

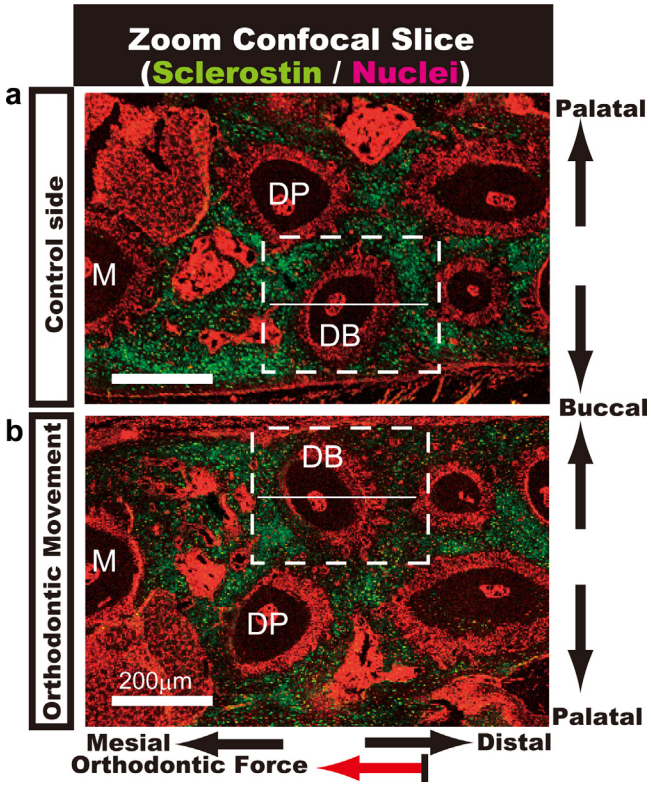

Figure 4 Magnified confocal images of immunofluorescence of sclerostin in the alveolar bone. Horizontal sections of alveolar bone were processed for immunofluorescence using anti-sclerostin antibodies (green) with nuclear counterstaining (red). (a, b) Optical slices obtained with zoom confocal microscopy on the control side (a) and orthodontic force side (b), respectively, are shown. The proximal-distal and palatal-buccal sides are indicated by horizontal and vertical black arrows, respectively. The red horizontal arrow indicates the direction of the orthodontic force. The white broken-lined rectangles highlight the distobuccal roots of the first molar, which are further quantitatively analyzed by three-dimensional fluorescence morphometry. Scale bars: 200 μm. (For interpretation of the references to color in this figure legend, the reader is referred to the web version of this article.)
Modified from Nishiyama et al., 2015 [Elsevier] [7].

fluorescence morphometry to analyze spatial changes in the sclerostin expression in the osteocytic lacunar—canalicular system in a mouse orthodontic tooth movement model (Fig. 4) [7]. Zoom confocal microscopy enables us to acquire wide views in the order of a few centimeters at a high resolution. Therefore, this system is advantageous to map local, site-specific changes in whole tissue. We successively employed a three-dimensional fluorescence morphometry analysis as described above and observed significant down-regulation of sclerostin in the osteocytic lacunar—canalicular system specifically in tensile sites of the alveolar bone, although the sclerostin signals in compression sites were significantly higher than those in the control site. The down-regulation of sclerostin in tensile sites favors subsequent bone formation through activating osteoblasts as a result of mechanical loading induced by orthodontic forces (Fig. 5). In compression sites, the up-regulation of

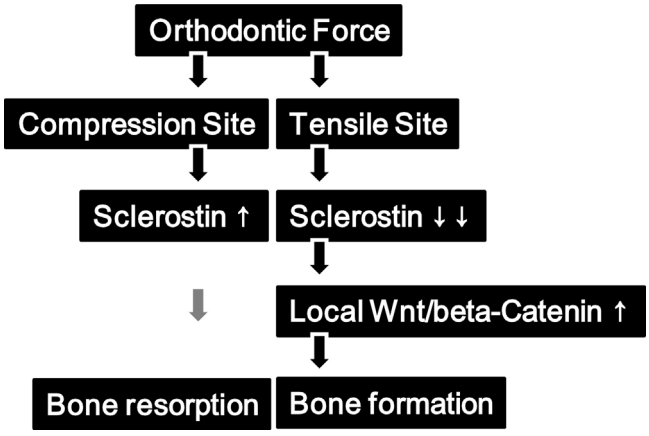

Figure 5 Site-specific regulation of sclerostin production by the orthodontic force. Sclerostin production by alveolar osteocytes is down-regulated and up-regulated in tensile and compression sites, respectively. A reduced production of sclerostin in tensile sites favors the activation of Wnt/beta-catenin signaling in adjacent osteoblasts, thus promoting bone formation to fill the alveolar space at this site.

sclerostin is induced by unloading or physiological tension release by local periodontal ligaments, thus inhibiting bone formation and making the bone prone to resorption at this bone site. These observations suggest that spatial changes in the level and distribution of sclerostin in the alveolar lacuna-canalicular system are a potent trigger for successive bone remodeling due to the orthodontic tooth. The multimodal confocal imaging analyses applied in this work enhances comprehensive understanding regarding the spatial regulation of molecules of interest from the tissue to the cellular level [7].

9. DMP1: a direct negative regulator of FGF23 production by osteocytes

FGF23, a member of fibroblast growth factor, is predominantly produced by osteocytes and hormonally regulates serum phosphate levels by targeting phosphate reabsorption in kidneys [24—29]. DMP1 is a non-collagenous extracellular matrix protein also produced by osteocytes and odontoblasts and regulates mineralization of the bone and dentin, respectively [30]. DMP1-deficient mice exhibited hyperphosphatemia through up-regulated FGF23 production, indicating that DMP1 is a negative regulator of FGF23 production [31]. The molecular mechanism underlying this phenotype, however, remains unclear.

To elucidate this issue, we first conducted double immunostaining of DMP1 and FGF23 in tissue sections of rat femurs and successive three-dimensional fluorescence morphometry (Fig. 6) [5]. The spatial distribution patterns and expression levels of DMP1 and FGF23 were observed to be inversely related, especially in cortical osteocytes. Specifically, in a single bone, DMP1-high or FGF23-high domains were designated. This finding, together with the genetic phenotype of DMP1-deficient bone, prompted us to postulate that DMP1 is a direct negative regulator of FGF23.

Inoculation of recombinant DMP1 protein to FGF23-producing osteoblasts showed significant down-regulation

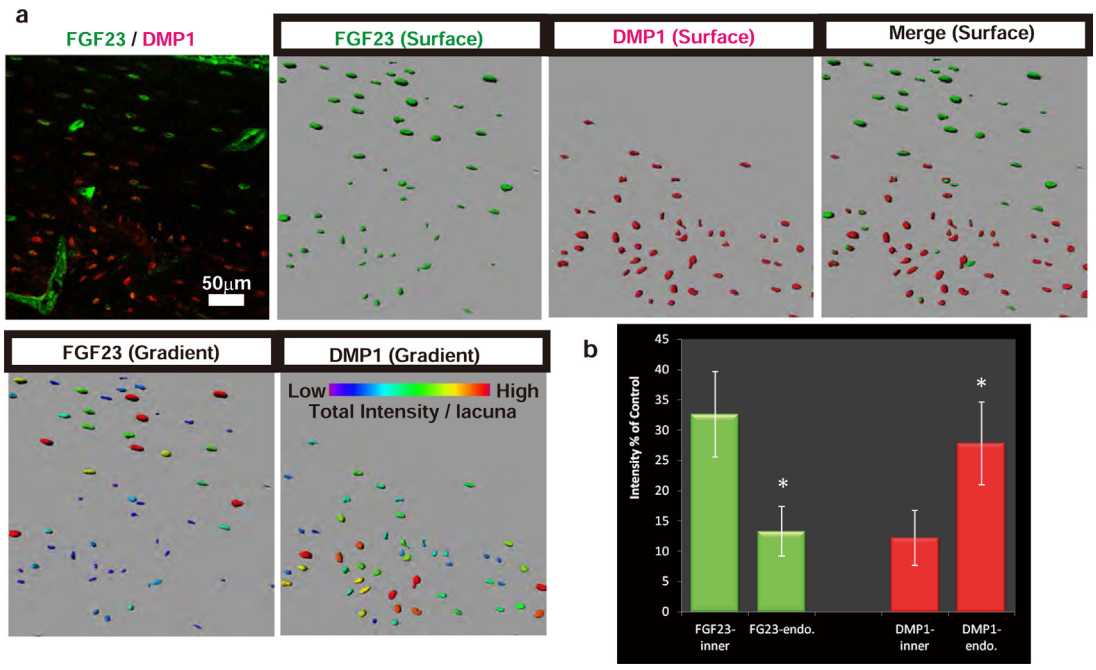

Figure 6 Distinct spatial distributions and the relative expression levels of FGF23 and DMP1 on three-dimensional (3D) immunofluorescence morphometry. (a) Tissue sections of the femurs of 16-week-old rats are stained with double immunofluorescence FGF23 (in green) and DMP1 (in red). Scale bar: 50 μm. An Easy 3D fluorescence image (upper left), surface rendering images of FGF23 (in green), DMP1 (in red), their merged image and the relative expression levels of FGF23 and DMP1 demonstrated by graded colors are shown. Scale bar: 50 μm. The endosteal side is on the bottom. (b) The relative fluorescence intensity of FGF23 and DMP1 in the inner portion and endosteal portion was statistically compared. (For interpretation of the references to color in this figure legend, the reader is referred to the web version of this article.)
Modified from Lee et al., 2014 [Nature publishing group] [5].

of FGF23 production in a dose-dependent manner, while positively regulating the extension of cellular processes [5]. Furthermore, molecular and cellular *in vitro* analyses demonstrated that negative regulation of FGF23 production and positive regulation of the extension of cellular processes by DMP1 were achieved *via* the FAK-MAPK pathway and the FAK-ROCK pathway, respectively (Fig. 7). Taken together, these findings obtained from *in vivo* quantitative fluorescence imaging and *in vitro* signaling analyses demonstrated that extracellular DMP1 conveys intracellular signaling pathways that regulate FGF23 production and osteocyte morphology [5].

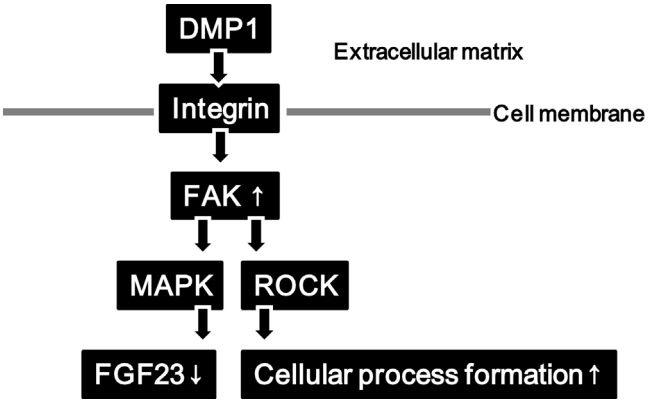

Figure 7 Regulatory signaling of osteocyte phenotypes mediated by extracellular DMP1. DMP1 binds to integrins and successively activates FAK. The FGF23 expression is downregulated by the FAK-MAPK pathway, while the FAK-ROCK pathway is positively involved in cytoskeletal reorganization and osteocytic cellular process formation.

10. Morphological and functional heterogeneity of osteocytes

Osteocytes are conventionally defined as a population of cells embedded in the mineralized bone matrix. However, the findings of osteocytes obtained by our quantitative fluorescence imaging approaches have provided a distinct view of osteocytes as a morphologically and functionally heterogenic population in bones [5]. Furthermore, this heterogeneity of osteocytes is possibly regulated by local mechanical loading and bone metabolism.

11. Future perspective

In this short review, quantitative fluorescence imaging approaches applied in skeletal tissue sections were discussed. The application of quantitative fluorescence imaging has enabled our research group to successfully uncover unprecedented biological phenomena. As described above, magnified imaging modalities, such as confocal tiling and zoom confocal imaging, are an effective approach to excluding the subjective selection of regions of interest

for further detailed image quantification. Therefore, multimodal imaging that combines several imaging modes at distinct magnifications and scale orders would be an extremely powerful tool to investigate molecular and cellular functions from the tissue to subcellular levels in a consistent manner. Now that super-resolution microscopy is being applied in biomedical science and provides imaging of unprecedented resolution (20—100 nm) [32], the application of multimodal imaging, including super-resolution microscopy, could become an attainable and powerful tool for biomedical and biodental science.

Needless to say, it is also important to understand the basic technology of fluorescence imaging and microscopy, in particular the technical limitations and biomedical application of the technique. Spectrum management of excitation wavelengths and characteristics of the fluorescence dye or fluorophore is a mandatory step to eliminate nonspecific signals from specific signals. It is also important to note that data acquired from quantitative fluoresce imaging should be fully supported or confirmed by other methods or previous literature to exclude misinterpretation of the acquired imaging data. The relevance of biological evaluations as well as optical knowledge is crucial to obtain novel insights by fluorescence imaging.

Image processing and mathematical analyses have remained ongoing subjects in the fluorescence imaging field. Live imaging-based embryonic body elongation and numerical analyses of tissue growth velocity have successfully unveiled novel regulatory mechanism by Hox genes for global body patterning [33]. Our current approach of fluorescence live imaging-based mathematical modeling is a powerful approach to unveil a tissue growth mode that is masked by a group of cells that exhibit stochastic functions [34].

Conflict of interest

The authors declare no conflicts of interest.

Role of funding source

The current work was supported by a Grant-in-Aid for Scientific Research from the Japan Society for the Promotion of Science (JSPS) (No. 26293392 and No. 26861549) of the Ministry of Education, Culture, Sports, Science, and Technology (MEXT) to T.I. and L.J-W., respectively.

Acknowledgements

The authors express sincere gratitude to Kazuaki Tokunaga, Satoshi Takiguchi and Norio Ohba at NikonInstech for their expertise in microscopy and image processing.

References

[1] Mavrakis M, Pourquie O, Lecuit T. Lighting up developmental mechanisms: how fluorescence imaging heralded a new era. Development 2010;137:373—87.
[2] Iimura T, Nakane A, Sugiyama M, Sato H, Makino Y, Watanabe T, et al. A fluorescence spotlight on the clockwork development and metabolism of bone. J Bone Miner Metab 2011;30:254—69.
[3] Schermelleh L, Heintzmann R, Leonhardt H. A guide to super-resolution fluorescence microscopy. J Cell Biol 2010;190:165—75.
[4] Himeno-Ando A, Izumi Y, Yamaguchi A, Iimura T. Structural differences in the osteocyte network between the calvaria and long bone revealed by three-dimensional fluorescence morphometry, possibly reflecting distinct mechano-adaptations and sensitivities. Biochem Biophys Res Commun 2012;417:765—70.
[5] Lee JW, Yamaguchi A, Iimura T. Functional heterogeneity of osteocytes in FGF23 production: the possible involvement of DMP1 as a direct negative regulator. BoneKEy Rep 2014;3:543.
[6] Makino Y, Takahashi Y, Tanabe R, Tamamura Y, Watanabe T, Haraikawa M, et al. Spatiotemporal disorder in the axial skeleton development of the Mesp2-null mouse: a model of spondylocostal dysostosis and spondylothoracic dysostosis. Bone 2013;53:248—58.
[7] Nishiyama Y, Matsumoto T, Lee JW, Saitou T, Imamura T, Moriyama K, et al. Changes in the spatial distribution of sclerostin in the osteocytic lacuno-canalicular system in alveolar bone due to orthodontic forces, as detected on multimodal confocal fluorescence imaging analyses. Arch Oral Biol 2015;60:45—54.
[8] Watanabe T, Tamamura Y, Hoshino A, Makino Y, Kamioka H, Amagasa T, et al. Increasing participation of sclerostin in postnatal bone development, revealed by three-dimensional immunofluorescence morphometry. Bone 2012;51:447—58.
[9] Kobayashi T, Kronenberg HM. Overview of skeletal development. Methods Mol Biol 2014;1130:3—12.
[10] Sakou T, Onishi T, Yamamoto T, Nagamine T, Sampath T, Ten Dijke P. Localization of Smads, the TGF-beta family intracellular signaling components during endochondral ossification. J Bone Miner Res 1999;14:1145—52.
[11] Serra R, Karaplis A, Sohn P. Parathyroid hormone-related peptide (PTHrP)-dependent and -independent effects of transforming growth factor beta (TGF-beta) on endochondral bone formation. J Cell Biol 1999;145:783—94.
[12] Ferguson CM, Schwarz EM, Reynolds PR, Puzas JE, Rosier RN, O'Keefe RJ. Smad2 and 3 mediate transforming growth factor-beta1-induced inhibition of chondrocyte maturation. Endocrinology 2000;141:4728—35.
[13] Seo HS, Serra R. Deletion of Tgfbr2 in Prx1-cre expressing mesenchyme results in defects in development of the long bones and joints. Dev Biol 2007;310:304—16.
[14] Minina E, Wenzel HM, Kreschel C, Karp S, Gaffield W, McMahon AP, et al. BMP and Ihh/PTHrP signaling interact to coordinate chondrocyte proliferation and differentiation. Development 2001;128:4523—34.
[15] Bonewald LF. The amazing osteocyte. J Bone Miner Res 2011;26:229—38.
[16] Schaffler MB, Cheung WY, Majeska R, Kennedy O. Osteocytes master orchestrators of bone. Calcif Tissue Int 2013.
[17] Poole KE, van Bezooijen RL, Loveridge N, Hamersma H, Papapoulos SE, Lowik CW, et al. Sclerostin is a delayed secreted product of osteocytes that inhibits bone formation. FASEB J 2005;19:1842—4.
[18] Winkler DG, Sutherland MK, Geoghegan JC, Yu C, Hayes T, Skonier JE, et al. Osteocyte control of bone formation via sclerostin, a novel BMP antagonist. EMBO J 2003;22:6267—76.
[19] van Bezooijen RL, Deruiter MC, Vilain N, Monteiro RM, Visser A, van der Wee-Pals L, et al. expression is restricted to the great arteries during embryonic and neonatal cardiovascular development. Dev Dyn 2007;236:606—12.
[20] van Bezooijen RL, Roelen BA, Visser A, van der Wee-Pals L, de Wilt E, Karperien M, et al. Sclerostin is an osteocyte-expressed negative regulator of bone formation, but not a classical BMP antagonist. J Exp Med 2004;199:805—14.

[21] van Bezooijen RL, ten Dijke P, Papapoulos SE, Lowik CW. SOST/sclerostin, an osteocyte-derived negative regulator of bone formation. Cytokine Growth Factor Rev 2005;16:319—27.
[22] ten Dijke P, Krause C, de Gorter DJ, Lowik CW, van Bezooijen RL. Osteocyte-derived sclerostin inhibits bone formation: its role in bone morphogenetic protein and Wnt signaling. J Bone Joint Surg Am 2008;90(Suppl 1):31—5.
[23] Matsumoto T, Iimura T, Ogura K, Moriyama K, Yamaguchi A. The role of osteocytes in bone resorption during orthodontic tooth movement. J Dent Res 2013;92:340—5.
[24] Weber TJ, Liu S, Indridason OS, Quarles LD. Serum FGF23 levels in normal and disordered phosphorus homeostasis. J Bone Miner Res 2003;18:1227—34.
[25] Shimada T, Kakitani M, Yamazaki Y, Hasegawa H, Takeuchi Y, Fujita T, et al. Targeted ablation of Fgf23 demonstrates an essential physiological role of FGF23 in phosphate and vitamin D metabolism. J Clin Invest 2004;113:561—8.
[26] Shimada T, Mizutani S, Muto T, Yoneya T, Hino R, Takeda S, et al. Cloning and characterization of FGF23 as a causative factor of tumor-induced osteomalacia. Proc Natl Acad Sci U S A 2001;98:6500—5.
[27] Liu S, Guo R, Simpson LG, Xiao ZS, Burnham CE, Quarles LD. Regulation of fibroblastic growth factor 23 expression but not degradation by PHEX. J Biol Chem 2003;278:37419—26.
[28] Sitara D, Razzaque MS, Hesse M, Yoganathan S, Taguchi T, Erben RG, et al. Homozygous ablation of fibroblast growth factor-23 results in hyperphosphatemia and impaired skeletogenesis, and reverses hypophosphatemia in Phex-deficient mice. Matrix Biol: J Int Soc Matrix Biol 2004;23:421—32.
[29] Gattineni J, Bates C, Twombley K, Dwarakanath V, Robinson ML, Goetz R, et al. FGF23 decreases renal NaPi-2a and NaPi-2c expression and induces hypophosphatemia in vivo predominantly via FGF receptor 1. Am J Physiol Renal Physiol 2009;297:F282—91.
[30] Toyosawa S, Shintani S, Fujiwara T, Ooshima T, Sato A, Ijuhin N, et al. Dentin matrix protein 1 is predominantly expressed in chicken and rat osteocytes but not in osteoblasts. J Bone Miner Res 2001;16:2017—26.
[31] Feng JQ, Ward LM, Liu S, Lu Y, Xie Y, Yuan B, et al. Loss of DMP1 causes rickets and osteomalacia and identifies a role for osteocytes in mineral metabolism. Nat Genet 2006;38:1310—5.
[32] Fornasiero EF, Opazo F. Super-resolution imaging for cell biologists: Concepts, applications, current challenges and developments. BioEssays: News Rev Mol Cell Dev Biol 2015.
[33] Denans N, Iimura T, Pourquie O. Hox genes control vertebrate body elongation by collinear Wnt repression. eLife 2015:2015.
[34] Sugiyama M, Saitou T, Kurokawa H, Sakaue-Sawano A, Imamura T, Miyawaki A, et al. Live imaging-based model selection reveals periodic regulation of the stochastic g1/s phase transition in vertebrate axial development. PLoS Comput Biol 2014;10:e1003957.